Supplementary Figures

Supplementary Fig. 1 Quality control of the scRNA-seq dataset and round 1 per-lineage reanalysis.
a, Schematic representation of the computational workflow used to analyse scRNA-seq data. **b,** UMAP projections of the scRNAseq data showing unbiased Louvain clusters, scrublet scores, sex, PCW, donor and given annotation for each cell. Dotplot showing the variance-scaled, log-transformed expression of marker genes in the main population. **c,** UMAP projections of the per-lineage scRNAseq reanalysis (round 1) showing unbiased Louvain clusters, sex, donor, PCW, cell cycle phase and scrublet scores for each cell in the germ, supporting, mesenchymal, epithelial and endothelial lineages.

Supplementary Fig. 2 Quality control of the scRNA-seq round 2 per-lineage reanalysis.
a, UMAP projections of the per-lineage scRNAseq reanalysis (round 2) showing unbiased Louvain clusters, sex, donor and PCW for each cell in the germ, supporting, mesenchymal, epithelial and endothelaial lineages. **b,** Dotplot showing the log-transformed expression of marker genes in the identified sub-populations for the mesenchymal, epithelial and endothelial lineages. Dotplots for germ and supporting cells are in Fig. 2 and Fig. 3-4, respectively.

Supplementary Fig. 3 Quality control of visium datasets and DSD genes.
a, H&E images matching the six tissue sections used for Visium spatial transcriptomics including two 11, 14 and 17 PCW ovaries and two 12 PCW testis. **b,** cell2location estimated amount of mRNA (colour intensity) contributed by each mesenchymal subpopulation to each Visium spot (colour) shown over the H&E images. **c**, Dotplot showing the variance-scaled, log-transformed expression of main DSD-associated genes in the identified gonadal populations. **d**, Heatmap showing the enrichment z-scores of the accessibility of transcription factor motifs associated with DSD with respect to the identified gonadal populations in scATAC-seq data from female (top) and male (bottom) samples.

Supplementary Fig. 4 Chromatin accessibility landscape of the developing ovaries and testes.
a, Schematic representation of the computational workflow used to analyse scATAC-seq data. **b,** UMAP projections of scATAC-seq data from female samples labeled by unbiased Leiden clustering, donor and PCW. **c**, Heatmap reporting label transfer scores from scRNA-seq to scATAC-seq data of matched individuals (females). **d**, UMAP projections of scATAC-seq data from male samples labeled by unbiased Leiden clustering, donor and PCW. **e**, UMAP projections of scATAC-seq data labeled by cell type identified in snRNA-seq data from the combined snRNA-seq/snATAC-seq profiling (males). Only gonads were included in the combined snRNA-seq/snATAC-seq assay. **f**, Heatmap showing enrichment z-scores for the top transcription factor (TF) motif per identified cell type in scATAC-seq data from female (left) and male samples (right). **g**, Hierarchical clustering of enrichment z-scores for peaks contained within each cis-co-accessibility network (CCAN) with respect to the cell types identified in scATAC-seq data from female (left) and male samples (right). **h**, Coverage plots of the genomic regions including the TFs *GATA4, LHX9, ARX, GATA2, NR2F1* with respect to the mesenchymal cell types identified in scATAC-seq data from female samples. **i,** Coverage plots of the genomic regions including the TFs *GATA4, LHX9, ARX, GATA2, NR2F1* with respect to the mesenchymal cell types identified in scATAC-seq data from male samples.

Supplementary Fig. 5 Spatial location, chromatin accessibility and cross species comparison of germ cells.

a, cell2location estimated amount of mRNA (colour intensity) contributed by each germ cell state to each Visium spot (colour) shown over the H&E image of 11, 14 and 17 PCW ovaries. **b,** cell2location estimated amount of mRNA (colour intensity) contributed by each germ cell state to each Visium spot (colour) shown over the H&E image of a 12 PCW testis. **c,** UMAP projections of scATAC-seq germ cells data labeled by unbiased Leiden clustering, sex, donor and PCW. **d**, Heatmap reporting label transfer scores from scRNA-seq to scATAC-seq germ cell data of matched individuals. **e**, UMAP projections of scATAC-seq data labeled by cell state identified in snRNA-seq germ cell data from the combined snRNA-seq/snATAC-seq profiling. **f**, Hierarchical clustering of enrichment z-scores for peaks contained within each cis-co-accessibility network (CCAN) with respect to the cell states identified in scATAC-seq germ cell data. **g**, UMAP projections of monkey ovarian germ cells re-analysed from Zhao *et al.*, 2020 labeled by cell state and developmental stage (E84 and E116). **h,** UMAP projections of mouse ovarian germ cells re-analysed from Niu and Spradling, 2020 labeled by cell state and developmental stage (E11.5 to P5). **i,** UMAP projections of mouse ovarian and testicular germ cells re-analysed from Mayere *et al.*, 2021 labeled by cell state and developmental stage (E10 to E16). **j**, Dot plot showing the log-transformed expression of known genes mediating oogenesis and spermatogenesis in mammalian germ cells from our human dataset, Zhao *et al.*, 2020, Niu and Spradling, 2020, Mayere *et al.*, 2021.

Supplementary Fig. 6 Supporting progenitor population.

a, Barplot showing the number of cells per identified supporting subpopulation classified by sex and PCW. **b,** Dot plot showing the log-transformed expression of DSD-associated genes characteristic of the sLGR5 subpopulation. **c,** High-resolution large-area imaging of representative gonadal sections of a human fetal testis (8PCW, CS20) and three fetal ovaries (7PCW, CS19), with intensity proportional to smFISH signal for *KLK11* (cyan), *LGR5* (yellow), *OSR1* or *SOX9* (red). **d** Dot plot showing the log-transformed expression of *SFRP1*, *SFRP2* and *AXIN2* in each supporting subpopulation.

Supplementary Fig. 7 sPAX8.

a, UMAP projections of scRNA-seq data from epithelials and sPAX8 cells (n = 10,794). **b,** UMAP coloured per donor, PCW and unbiased Louvain clustering. **c,** Barplot showing the number of cells per subpopulation classified by sex and PCW. **d,** Dot plot showing the log-transformed expression of genes characteristic of the epithelial and sPAX8 cell states. **e,** High-resolution imaging of representative gonadal sections of three human fetal testes (8, 11 and 12 PCW), with intensity proportional to smFISH signal for *EPCAM* (red), *PAX8* (yellow), *NR5A1* (cyan) and *KLK11* (green). White dashed rectangles highlight enlarged gonadal regions with PAX8^{high}/EPCAM^{low} expression; Mesonephric tubules (*EPCAM*^{high},PAX8+) marked with white asterisk. Scale bars = 100um. **f,** High-resolution imaging of representative gonadal sections of three fetal ovaries (9, 11 and 14 PCW), with intensity proportional to smFISH signal for *EPCAM* (red), *NR5A1* (cyan), *KLK11* (green) and *PAX8* (yellow). White dashed rectangles highlight enlarged gonadal regions with *PAX8*^{high}/*EPCAM*^{low} expression. Scale bars = 100um unless specified. **g,** UMAP projections of mouse ovarian supporting cells re-analysed from Niu and Spradling, 2020 labeled by cell state and developmental stage (E11.5 to P5) **h,** UMAP projections of mouse ovarian supporting cells re-analysed from Niu and Spradling, 2020 showing the label transfer probabilities for sPAX8e using a SVM model

trained on human ovarian supporting cells. **i,** UMAP projections of mouse ovarian supporting cells re-analysed from Niu and Spradling, 2020 showing the log-transformed expression of Pax8, Lypd1, Txb1, Tbx2, Aldh1a3 and Pdgfrl. **j,** High-resolution large-area imaging of one mouse fetal ovary (E13.5), with intensity proportional to smFISH signal for Lgr5 (yellow), Pax8 (red), Hmgcs2 (green, pre-granulosa medullary marker) and Gng13 (purple, pre-granulosa cortical marker). White dashed rectangles highlight enlarged gonadal regions with $PAX8^{high}/EPCAM^{low}$ expression. Scale bars = 100um. MD = Mullerian Duct.

Supplementary Fig. 8 Spatial location, chromatin accessibility and cross species comparison of supporting cells.
a, cell2location estimated amount of mRNA (colour intensity) contributed by each preGC-II (preGCa/b/c) and developing granulosa population to each Visium spot (colour) shown over the H&E image of a 11, 14 and 17 PCW ovaries. **b**, UMAP projections of scATAC-seq supporting cells data labeled unbiased Leiden clustering, sex, donor and PCW. **c,** Heatmap reporting label transfer scores from scRNA-seq to scATAC-seq supporting cells data of matched individuals. **d**, UMAP projections of scATAC-seq data labeled by cell state identified in snRNA-seq supporting cells data from the combined snRNA-seq/snATAC-seq profiling. **e**, UMAP projections of monkey ovarian supporting cells re-analysed from Zhao *et al*., 2020 labeled by cell state and developmental stage (E84 and E116). **f**, UMAP projections of monkey ovarian supporting cells re-analysed from Zhao *et al*, 2020 showing the label transfer probabilities using a SVM model trained on human ovarian supporting cells. **g**, UMAP projections of mouse ovarian supporting cells re-analysed from Niu and Spradling, 2020 labeled by cell state and developmental stage (E11.5 to P5). **h**, UMAP projections of mouse ovarian supporting cells re-analysed from Niu and Spradling, 2020 showing the label transfer probabilities using a SVM model trained on human ovarian supporting cells. **i**, UMAP projections of mouse ovarian supporting cells re-analysed from Niu and Spradling, 2020 showing the log-transformed expression of *LGR5* (mouse marker of cortical pre-granulosa) and *FOXL2* (mouse marker of medullary pre-granulosa). **j**, UMAP projections of mouse ovarian supporting cells re-analysed from Niu and Spradling, 2020 showing the log-transformed expression of functional markers of the two waves of pre-granulosa cells which are conserved across species.

Supplementary Fig. 9 Tissue-resident macrophages in the developing testes. a, Schematics illustrating the CD45+ enrichment strategy for gonadal and extragonadal samples. **b,** UMAP projections of immune cells labeled by unbiased Leiden clustering, sex, donor and PCW. **c,** Heatmap showing label transfer scores from the fetal liver hematopoiesis dataset (Popescu *et al*., 2019) to our gonadal immune dataset using a Support Vector Machine (SVM) classifier. Low probabilities assigned to neutrophils, which were not defined in the liver dataset, and to macrophages **d,** Dot plot showing variance-scaled, log-transformed expression of marker genes expressed in the identified immune subsets. **e,** Bar plot showcasing the proportion of cells belonging to the main immune lineages during the first and second trimester of pregnancy. **f**, Transcription factor activities computed with Dorothea for the identified macrophage subsets. **g,** Representative Gene Ontology (Biological Process) enriched terms for the identified macrophages subsets. **h,** UMAP projections of the multi-organ integrated fetal myeloid dataset labeled by unbiased Leiden clustering, donor and tissue. **i,** Dot plot showing variance-scaled, log-transformed expression of marker genes expressed in the identified cell populations from the multi-organ integrated fetal myeloid dataset.

Supplementary Fig. 10 Macrophages smFISH panels

a, High-resolution imaging of representative gonadal sections of a fetal ovary (14 PCW) and a fetal testis (12PCW), with intensity proportional to smFISH signal to *EPCAM* (cyan, high = epithelial cells; low = sertoli and germ cells), *CD68* (red, macrophages), *F13A1* (yellow, tissue-repair macrophages). White dashed rectangles highlight gonadal regions magnified. **b,** High-resolution imaging of representative gonadal sections of three fetal testes (11, 12 and 19 PCW), with intensity proportional to smFISH signal to *PDGFRA* (green, mesenchymal), *EPCAM* (cyan, high = epithelial cells; low = sertoli and germ cells), CD68 (red, macrophages), *SIGLEC15* (yellow, *SIGLEC15*+ macrophages). White dashed rectangles highlight gonadal regions magnified. **c,** High-resolution imaging of representative gonadal sections of three fetal testes (8, 14 and 15 PCW), with intensity proportional to smFISH signal to *PDGFRA* (green, mesenchymal), *CDH5* (cyan, endothelial cells), *CD68* (red, macrophages), *SIGLEC15* (yellow, *SIGLEC15*+ macrophages). White dashed rectangles highlight gonadal regions magnified. **d,** High-resolution imaging of representative gonadal sections of two fetal testes (12 PCW), with intensity proportional to smFISH signal to *SOX9* (purple, Sertoli cells), *CD68* (red, macrophages), *P2RY12* (yellow, microglia-like macrophages). White dashed rectangles highlight gonadal regions magnified. **E,** High-resolution imaging of a representative gonadal sections of fetal testis (12 PCW), with intensity proportional to smFISH signal to *PDGFRA* (cyan, mesenchymal), *POU5F1* (purple, primordial germ cells), *CD68* (red, macrophages), *P2RY12* (yellow, microglia-like macrophages). White dashed rectangles highlight gonadal regions magnified.

Scale bars =100um unless indicated

Supplementary Tables

Supplementary Table 1

Metadata of samples.

Sample = 10x reaction; Individual = Individual ID; Stage = Post Conceptional Weeks; Sex = female or male detemined by karyotype and sequencing; Process = total (no enrichment); CD45- (non-immune fraction); cryo = yes, if cryopreserved; TP = type of pregnancy termination (Med: medical, or Sur: surgical); 10x kit = 5' reaction (v1 or v2); scATAC-seq; or multiomics kit.

scRNA-seq:

sample	individual	Stage (PCW)	Stage (CS)	sex	batch_collection	process	cryo	TP	10x kit
FCA_GND8047885	F81	8.8	23	female	A	CD45-	No	Med	5' v1
FCA_GND8047884	F81	8.8	23	female	A	CD45+	No	Med	5' v1
FCA_GND8125923	F86	7.5	19	female	B	CD45-	No	Med	5' v1
FCA_GND8125922	F86	7.5	19	female	B	CD45+	No	Med	5' v1
FCA_GND8125925	F87	11		female	B	CD45-	No	Med	5' v1
FCA_GND8125924	F87	11		female	B	CD45+	No	Med	5' v1
FCA_GND8103050	F83	17		female	C	CD45-	No	Med	5' v1
FCA_GND8103049	F83	17		female	C	CD45+	No	Med	5' v1
FCA_GND8103053	F84	9		female	C	CD45-	No	Med	5' v1
FCA_GND8103052	F84	9		female	C	CD45+	No	Med	5' v1
FCA_GND8289579	F88	11		male	D	CD45+	No	Med	5' v1
FCA_GND8622625	F89	8.4	22	female	E	total	No	Med	5' v1
FCA_GND8622626	F89	8.4	22	female	E	total	No	Med	5' v1
FCA_GND8622628	F91	11		female	E	CD45-	No	Med	5' v1
FCA_GND8622627	F91	11		female	E	CD45+	No	Med	5' v1
FCA_GND8622629	F93	6	16	female	E	CD45+	No	Med	5' v1
FCA_GND8622631	F94	12		male	E	CD45+	No	Med	5' v1
FCA_GND8715408	F96	14		female	F	CD45-	No	Med	5' v1
FCA_GND8289580	F88	11		male	D	CD45-	No	Med	5' v1
FCA_GND8622630	F93	6		male	E	CD45-	No	Med	5' v1
FCA_GND8715407	F96	14		female	F	CD45+	No	Med	5' v1

FCA_GND8784459	F99	8.6		female	H	CD45+	No	Med	5' v1
FCA_GND8715519	Hrv3	19		male	G	total	No	Med	5' v1
FCA_GND8784460	F99	8.6	23	female	H	CD45-	No	Med	5' v1
FCA_GND8784458	Hrv10	9		male	H	total	No	Med	5' v1
FCA_GND8810844	Hrv11	14		female	I	total	No	Med	5' v1
FCA_GND8810845	Hrv12	8.6	23	female	I	total	No	Sur	5' v1
FCA_GND8810848	Hrv13	9		female	I	total	No	Med	5' v1
FCA_GND8810846	Hrv15	12		male	I	total	No	Med	5' v1
FCA_GND8810850	Hrv16	7	18	male	I	total	No	Med	5' v1
FCA_GND8810851	Hrv17	7	18	male	I	total	No	Med	5' v1
FCA_GND8810852	Hrv18	12		male	I	total	No	Med	5' v1
FCA_GND9331965	Hrv30	12		female	J	total	No	Sur	5' v1
FCA_GND9331966	Hrv32	12		male	J	total	No	Sur	5' v1
FCA_GND9331967	Hrv33	15		male	J	total	No	Sur	5' v1
FCA_GND9331968	Hrv34	16		female	J	total	No	Sur	5' v1
FCA_GND9331969	Hrv31	11		male	J	total	Yes	Sur	5' v1
FCA_GND9331970	Hrv25	14		male	J	total	Yes	Sur	5' v1
FCA_GND9295208	F100	16		male	K	total	No	Med	5' v1
FCA_GND9295209	F100	16		male	K	total	No	Med	5' v1
FCA_GND9295210	Hrv21	17		male	K	total	No	Sur	5' v1
FCA_GND9295212	Hrv27	14		male	K	total	No	Sur	5' v1
FCA_GND9332062	F122	15		male	L	total	No	Med	5' v1
FCA_GND9332064	F123	6	16	female	L	total	No	Med	5' v1
FCA_GND9332065	F123	6	16	female	L	total	No	Med	5' v1
FCA_GND9332061	Hrv34	16		female	L	total	No	U	5' v1
HD_F_GON9460406	Hrv37	10		female	M	total	No	Sur	5' v1
HD_F_GON9460407	Hrv37	10		female	M	total	No	Sur	5' v1
HD_F_GON9460408	Hrv41	8.6	23	male	M	total	Yes	U	5' v1
HD_F_GON9480063	Hrv49	13		female	N	total	No	Sur	5' v1
HD_F_GON9480064	Hrv49	13		female	N	total	No	Sur	5' v1
HD_F_GON9480066	Hrv47	8.6	23	female	N	total	Yes	Sur	5' v1
HD_F_GON9479968	F126	9		female	N	total	No	Sur	5' v1

HD_F_GON9479969	Hrv39	14		female	N	total	Yes	Sur	5' v1
HD_F_GON9479970	Hrv40	15		male	N	total	No	Sur	5' v1
HD_F_GON9699334	Hrv58	21		female	O	total	No	Sur	5' v2
HD_F_GON9699332	Hrv58	21		female	O	total	No	Sur	5' v2
HD_F_GON9699337	Hrv59	18		female	O	total	No	Sur	5' v2
HD_F_GON9883867	Hrv58	21		female	O	total	No	Sur	5' v1
HD_F_GON9883866	Hrv59	18		female	O	total	No	Sur	5' v1
HD_F_GON9883862	F133	17		female	O	total	No	Sur	5' v1
HD_F_GON9883863	F133	17		female	O	total	No	Sur	5' v1
HD_F_GON9883859	Hrv55	17		male	O	total	No	Sur	5' v1
HD_F_GON9883868	Hrv54	21		male	O	total	No	Sur	5' v1

scATAC-seq:

sample	**individual**	**Stage (PCW)**	**Stage (CS)**	**sex**	**batch_collection**	**process**	**cryo**	**TP**	**10x kit**
FCA_GND8046539	F81	8.8	23	female	A	total	No	Med	ATAC v1
HD_F_GON9479873	Hrv49	13		female	N	total	No	Sur	ATAC v1
HD_F_GON9479874	Hrv50	14		female	N/A	total	No	Sur	ATAC v1
HD_F_GON9479871	Hrv39	14		female	N	total	Yes	Sur	ATAC v1
HD_F_GON9479872	Hrv40	15		male	N	total	Yes	Sur	ATAC v1
FCA_GND8768485	Hrv13	9		female	I	total	No	Med	ATAC v1
HD_F_GON9479875	Hrv50	14		female	N/A	total	No	Sur	ATAC v1
FCA_GND8795927	Hrv17	7	18	male	I	total	No	Med	ATAC v1
FCA_GND9332157	Hrv21	17		male	K	total	No	Sur	ATAC v1
FCA_GND8795928	Hrv18	12		male	I	total	No	Med	ATAC v1
FCA_GND8768484	Hrv12	8.6	23	female	I	total	No	Sur	ATAC v1
HD_F_GON9883959	Hrv59	18		female	O	total	No	Sur	ATAC v1
HD_F_GON9525612	Hrv15	12		male	I	total	No	Med	multiomics
HD_F_GON9525611	Hrv15	12		male	I	total	No	Med	multiomics
FCA_GND8768482	Hrv10	9		male	H	total	No	Med	ATAC v1
HD_F_GON9883960	Hrv58	21		female	O	total	No	Sur	ATAC v1

FCA_GND8768481	Hrv3	19		male	G	total	No	Med	ATAC v1
FCA_GND8768483	Hrv11	14		female	I	total	No	Med	ATAC v1
HD_F_GON9525614	Hrv39	14		female	N	total	Yes	Sur	multiomics
FCA_GND8768487	Hrv15	12		male	I	total	No	Med	ATAC v1
HD_F_GON9525613	Hrv39	14		female	N	total	Yes	Sur	multiomics

Supplementary Table 2. Supplementary_Table2.xlsx (separate file)
Quality control of samples. (1) Table containing summary statistics from 10x Cell Ranger 3.1.0 for each 10x scRNAseq library in our fetal gonads atlas. (2) Table containing summary statistics for each barcode passing QC filters. (3) Table containing summary statistics from 10x Cell Ranger ATAC 1.2 for each 10x scATACseq library in our fetal gonads atlas.

Supplementary Table 3. Supplementary_Table3.xlsx (separate file)
(1) Table containing differentially expressed genes computed with TF-IDF in the main cell types identified in our fetal gonads atlas.

Supplementary Table 4. Supplementary_Table4.xlsx (separate file)
(1) Table containing cis-co-accessibility networks computed with Cicero from scATAC-seq data of female samples. Accessible peaks (rows) are grouped in cis-co-accessibility networks (CCANs). For each CCAN we report an enrichment z-score with respect to the identified cell types. (2) Table containing enrichment z-scores of the TF motif activities computed with chromVar with respect to the identified cell types in scATAC-seq data of female samples. (3) Table containing cis-co-accessibility networks computed with Cicero from scATAC-seq data of male samples. Accessible peaks (rows) are grouped in cis-co-accessibility networks (CCANs). For each CCAN we report an enrichment z-score with respect to the identified cell types. (4) Table containing enrichment z-scores of the TF motif activities computed with chromVar with respect to the identified cell types in scATAC-seq data of male samples.

Supplementary Table 5. Supplementary_Table5.xlsx (separate file)
(1) Table containing differentially expressed genes in the main germ cell subsets. Each row represents a gene/cluster analysis. (2) Table containing differential Dorothea TF activities estimated in the germ cell subpopulations in scRNA-seq dataset. Each row represents a TF/cluster analysis. (3) Table containing TF binding activities estimated in the germ cell subpopulations from scATAC-seq data. (4) Integration of different TFs measurements. (5) Table containing cis-co-accessibility networks computed with Cicero from scATAC-seq data from germ cells. Accessible peaks (rows) are grouped in cis-co-accessibility networks (CCANs). For each CCAN we report an enrichment z-score with respect to the identified germ cell states.

Supplementary Table 6. Supplementary_Table6.xlsx (separate file)
(1) Table containing differentially expressed genes computed with TF-IDF in the main cell types identified in the fetal ovarian macaque dataset from Zhao *et al*., 2020. (2) Table containing differentially expressed genes computed with TF-IDF in the main cell types in the fetal ovarian mouse dataset from Niu and Spradling, 2020. (3) Table containing differentially

expressed genes computed with TF-IDF in the germ cell states identified in the fetal gonadal dataset from Mayere *et al*., 2021.

Supplementary Table 7. Supplementary_Table7.xlsx (separate file)
(1) Table containing differentially expressed genes within the supporting subpopulations computed with TF-IDF. (2) Table containing differentially expressed genes between males and females (sexually dimorphic genes) in the sLGR5 cells. Each row represents a gene/cluster analysis. (3) Table containing cis-co-accessibility networks computed with Cicero from scATAC-seq data from supporting cells. Accessible peaks (rows) are grouped in cis-co-accessibility networks (CCANs). For each CCAN we report an enrichment z-score with respect to the identified supporting subpopulations.

Supplementary Table 8. Supplementary_Table8.xlsx (separate file)
(1) CellPhoneDB interactions (germ-sertoli lineage cells). Columns represent interaction cell pairs, rows represent the interactions. Table is binary, with 1 indicating that all the members of the interaction are expressed in at least 10% cells and at least one member is a DEGs with a log2-fold change above 0.02 and adjusted p-value < 0.001. (2) Interactions in Figure 3f.

Supplementary Table 9. Supplementary_Table9.xlsx (separate file)
(1) Table containing SVM predictions on macaque ovarian supporting cells from human ovarian supporting cells. (2) Table containing SVM predictions on mouse ovarian supporting cells from human ovarian supporting cells.

Supplementary Table 10. Supplementary_Table10.xlsx (separate file)
(1) Table containing differentially expressed genes in the supporting subpopulations. Each row represents a gene/cluster analysis. (2) Table containing differential Dorothea TF activities estimated in the supporting subpopulations in scRNA-seq dataset. Each row represents a TF/cluster analysis. (3) Table containing TF binding activities estimated in the supporting subpopulations from scATAC-seq data. (4) Integration of different TFs measurements.

Supplementary Table 11. Supplementary_Table11.xlsx (separate file)
(1) CellPhoneDB interactions (germ-granulosa lineage and coelomic epithelial cells). Columns represent interaction cell pairs, rows represent the interactions. Table is binary, with 1 indicating that all the members of the interaction are expressed in at least 10% cells and at least one member is a DEGs with a log2-fold change above 0.02 and adjusted p-value < 0.001. (2) Interactions in Figure 5.

Supplementary Table 12. Supplementary_Table12.xlsx (separate file)
(1) Table containing differentially expressed genes in the immune dataset computed with TF-IDF. (2) SVM predictions on the immune populations from the fetal liver immune dataset (Popescu *et al.*, 2019).

Supplementary Table 13. Supplementary_Table13.xlsx (separate file)
(1) Table containing differentially expressed genes in the macrophage subsets computed with TF-IDF. (2) SVM predictions on the immune populations from the fetal macrophages dataset containing microglia (Bian *et al.*, 2020). The cluster of microglia from Bian *et al.*, 2020 is labeled as “Mac_4”. (3) Table containing Dorothea TF activities estimated in the macrophage

subsets. (5) Gene Ontology (Biological Process) enriched terms (top 100) for the cluster of tissue-repair macrophages. (6) Gene Ontology (Biological Process) enriched terms (top 100) for the cluster of ifn-induced macrophages. (7) Gene Ontology (Biological process) enriched terms (top 100) for the cluster of microglia-like macrophages. (8) Gene Ontology (Biological Process) enriched terms (top 100) for the cluster of *SIGLEC15*+ macrophages. (9) Table containing differentially expressed genes in the populations identified in the fetal multi-organ myeloid dataset computed with TF-IDF.

Supplementary Table 14. Supplementary_Table14.xlsx (separate file)
(1) Table containing CellPhoneDB interactions predicted for macrophage subsets and other gonadal testicular populations. Columns represent interaction cell pairs, rows represent the interactions. Table is binary, with 1 indicating that all the members of the interaction are expressed in at least 10% and at least one member is a DEGs in any cell-type in the pair with a positive log-fold change with FDR < 0.001. (2) Interactions in Figure 6.

Supplementary Table 15.
RNAscope probes.

TARGET GENE	PROBE	SUPPLIER	PRODUCT NUMBER
CD68	RNAscope 2.5 LS Probe Hs-CD68-C3	ACD, Bio-Techne	560598-C3
CD68	RNAscope 2.5 LS Probe Hs-CD68-C4	ACD, Bio-Techne	560598-C4
CDH5	RNAscope 2.5 LS Probe Hs-CDH5-C4	ACD, Bio-Techne	437458-C4
DAZL	RNAscope 2.5 LS Probe Hs-DAZL-C4	ACD, Bio-Techne	886978-C4
EPCAM	RNAscope 2.5 LS Probe Hs-EPCAM-C4	ACD, Bio-Techne	310288-C4
F13A1	RNAscope 2.5 LS Probe Hs-F13A1	ACD, Bio-Techne	433598
FIGLA	RNAscope 2.5 LS Probe Hs-FIGLA	ACD, Bio-Techne	1030238
KLK11	RNAscope 2.5 LS Probe Hs-KLK11	ACD, Bio-Techne	528808
LGR5	RNAscope 2.5 LS Probe Hs-LGR5	ACD, Bio-Techne	311028
LGR5	RNAscope 2.5 LS Probe Hs-LGR5-C2	ACD, Bio-Techne	311028-C2
LGR5	RNAscope 2.5 LS Probe Hs-LGR5-C3	ACD, Bio-Techne	311028-C3
OSR1	RNAscope 2.5 LS Probe Hs-OSR1-C4	ACD, Bio-Techne	1030268-C4
P2RY12	RNAscope 2.5 LS Probe Hs-P2RY12-C2	ACD, Bio-Techne	450398-C2
PAX8	RNAscope 2.5 LS Probe Hs-PAX8-C2	ACD, Bio-Techne	402368-C2
PDGFRA	RNAscope 2.5 LS Probe Hs-PDGFRA-C2	ACD, Bio-Techne	604488-C2

POU5F1	RNAscope 2.5 LS Probe Hs-POU5F1-C3	ACD, Bio-Techne	592868-C3
SIGLEC15	RNAscope 2.5 LS Probe Hs-SIGLEC15	ACD, Bio-Techne	527888
SOX9	RNAscope 2.5 LS Probe Hs-SOX9-C3	ACD, Bio-Techne	518668-C3
Gng13	RNAscope 2.5 LS Probe Mm-Gng13	ACD, Bio-Techne	462538-C4
Hmgcs2	RNAscope 2.5 LS Probe Mm-Hmgcs2	ACD, Bio-Techne	437148
Lgr5	RNAscope 2.5 LS Probe Mm-Lgr5-C3	ACD, Bio-Techne	312178-C3
Pax8	RNAscope 2.5 LS Probe Mm-Pax8-C2	ACD, Bio-Techne	574438-C2

Supplementary Table 16.
(1) New manually curated L-Rinteractions. (2) Complexes involved in the novel CellphoneDB interactions. (3) CellSign: new manually curated Receptor-TF interactions.

a scRNAseq analysis pipeline

10x Cell Ranger v 3.1.0
(1) reads alignement
(2) gene quantification
(3) barcode cell calling

359,561 cells

→

QC filtering
(1) cells >= 300 genes
(2) genes >= 3 cells
(3) cells <= 20% mitochondrial genes
(4) Sex annotation

319,081 cells

→

Cell Clustering
(1) Dimentionality reduction
(2) Individuals integration w/ Harmony
(3) Clustering w/ Louvain

→

Cluster characterization
(1) Identification of cluster-specific genes w/ TF-IDF
(2) Low QC & cycling cluster labelling
(3) Doublets identification w/ scrublet

247,842 cells

Zoom-in re-analysis per lineage

(round1) high resolution clustering to identify lowQC and doublet clusters

(round 2) re-clustering with high confident cells

65 cell states

b scRNAseq analysis

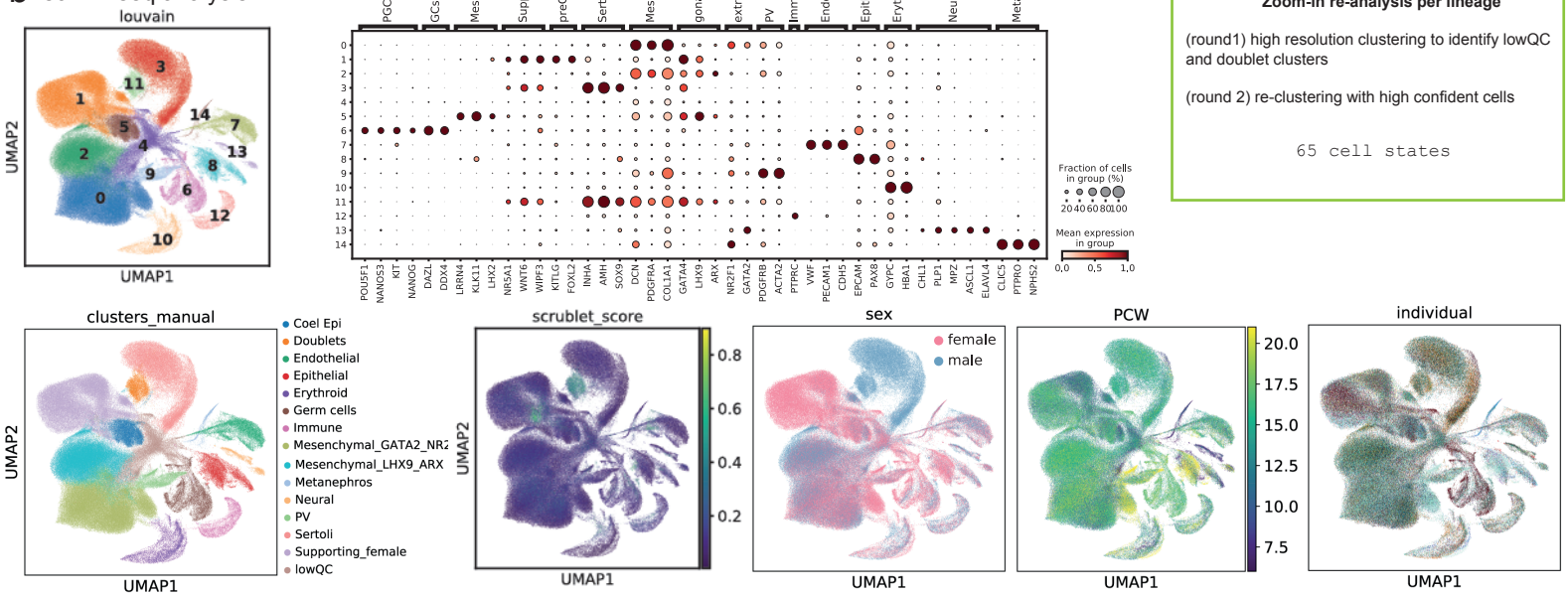

c scRNAseq -re-analysis of main lineages (round 1)

GERM CELLS

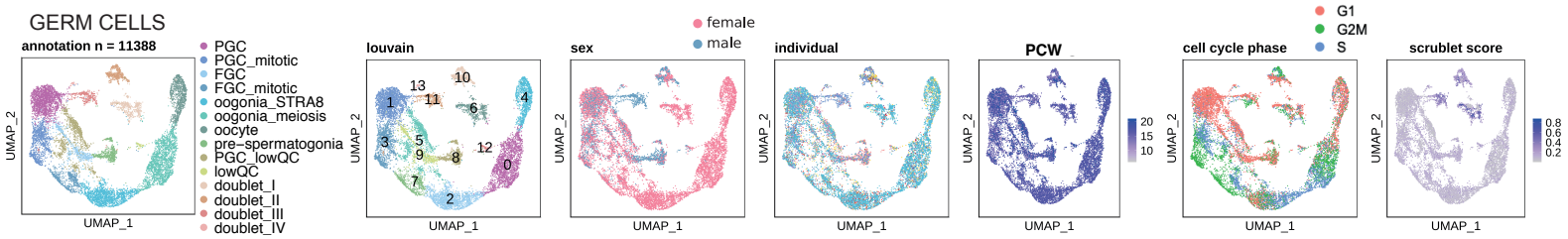

SUPPORTING CELLS

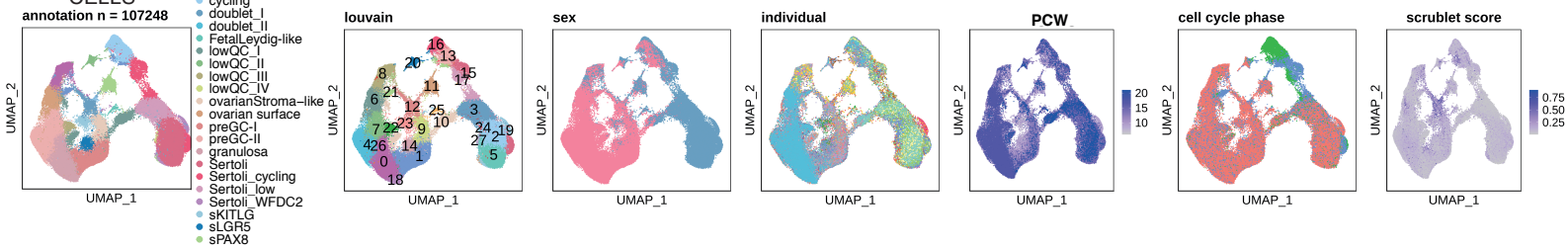

MESENCHYMAL CELLS

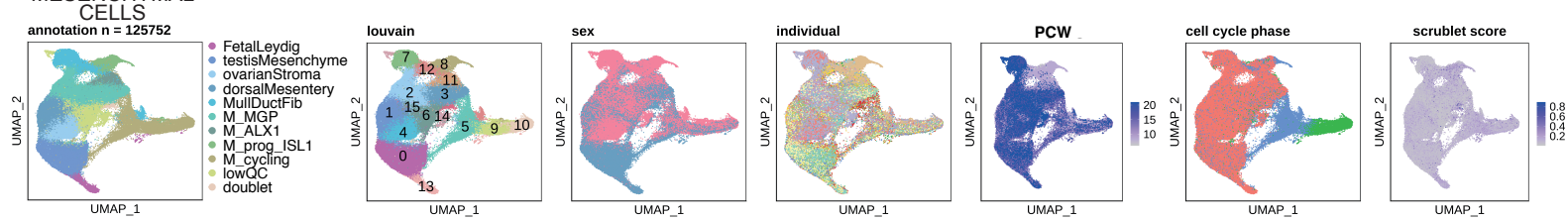

ENDOTHELIAL CELLS

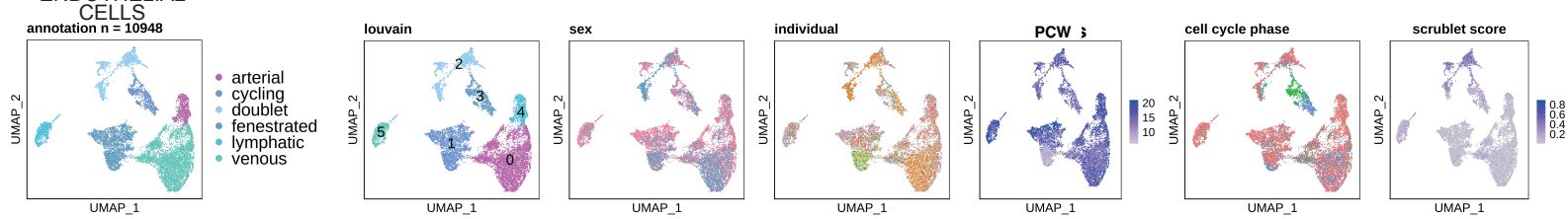

EPITHELIAL CELLS

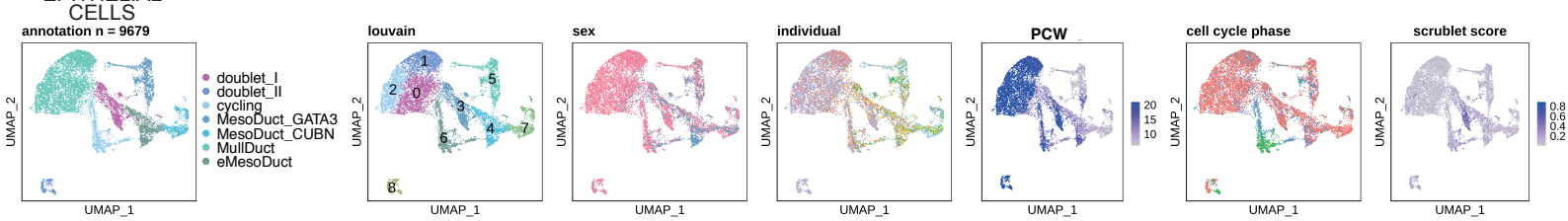

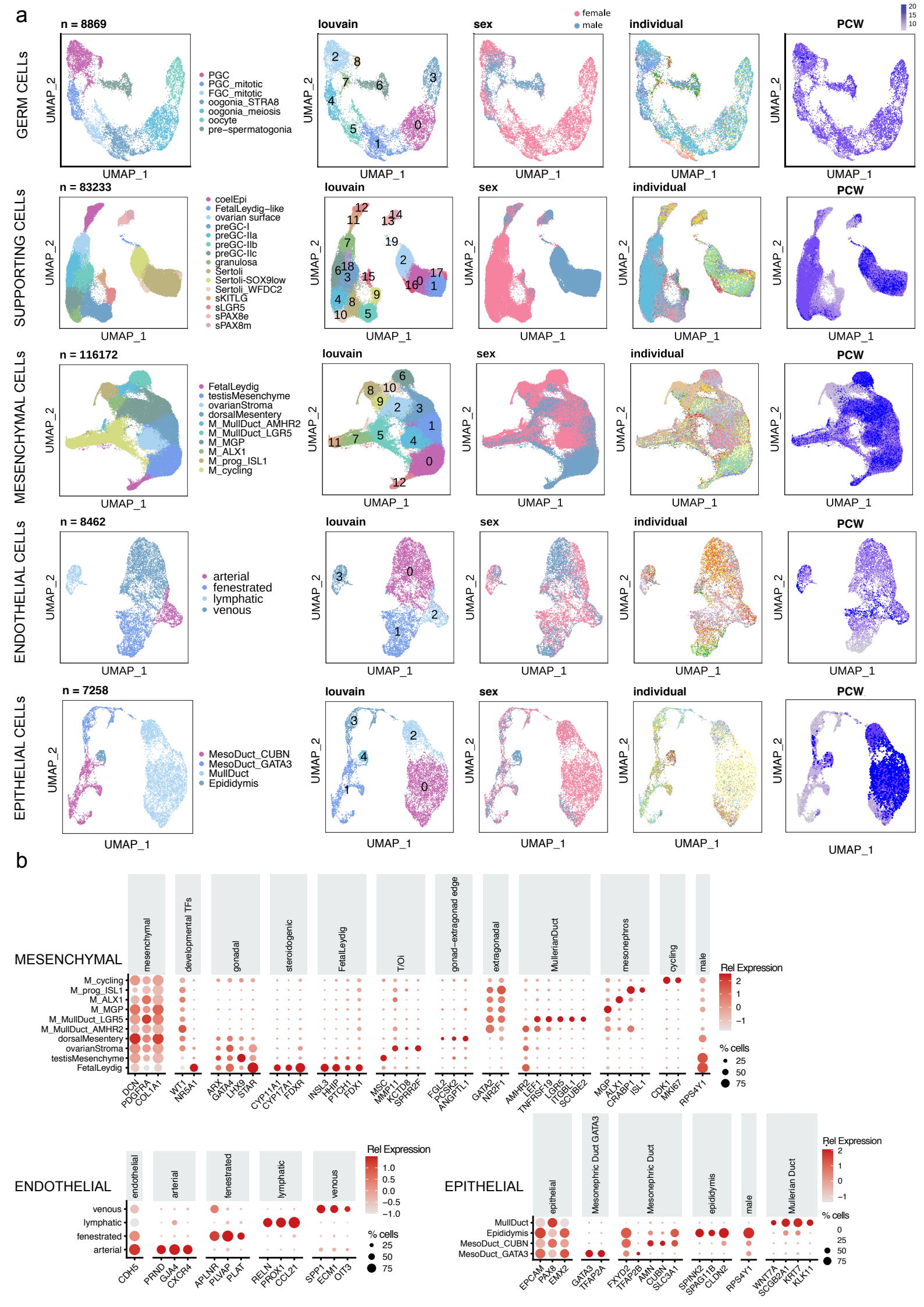
a
GERM CELLS
n = 8869
PGC
PGC_mitotic
FGC_mitotic
oogonia_STRA8
oogonia_meiosis
oocyte
pre−spermatogonia
louvain
sex
female
male
individual
PCW
SUPPORTING CELLS
n = 83233
coelEpi
FetalLeydig−like
ovarian surface
preGC−I
preGC−IIa
preGC−IIb
preGC−IIc
granulosa
Sertoli
Sertoli−SOX9low
Sertoli_WFDC2
sKITLG
sLGR5
sPAX8e
sPAX8m
MESENCHYMAL CELLS
n = 116172
FetalLeydig
testisMesenchyme
ovarianStroma
dorsalMesentery
M_MullDuct_AMHR2
M_MullDuct_LGR5
M_MGP
M_ALX1
M_prog_ISL1
M_cycling
ENDOTHELIAL CELLS
n = 8462
arterial
fenestrated
lymphatic
venous
EPITHELIAL CELLS
n = 7258
MesoDuct_CUBN
MesoDuct_GATA3
MullDuct
Epididymis
UMAP_1
UMAP_2
b
MESENCHYMAL
mesenchymal
developmental TFs
gonadal
steroidogenic
FetalLeydig
T/Oi
gonad−extragonad edge
extragonadal
MullerianDuct
mesonephros
cycling
male
M_cycling
M_prog_ISL1
M_ALX1
M_MGP
M_MullDuct_LGR5
M_MullDuct_AMHR2
dorsalMesentery
ovarianStroma
testisMesenchyme
FetalLeydig
DCN PDGFRA COL1A1
WT1 NR5A1
ARX GATA4 LHX9 STAR
CYP11A1 CYP17A1 FDXR
INSL3 HHIP PTCH1 FDX1
MSC MMP11 KCTD8 SPRR2F
FGL2 PCSK2 ANGPTL1
GATA2 NR2F1
AMHR2 LEF1 TNFRSF19 LGR5 ITGBL1 SCUBE2
MGP ALX1 CRABP1 ISL1
CDK1 MKI67
RPS4Y1
Rel Expression
2
1
0
−1
% cells
25
50
75
ENDOTHELIAL
endothelial
arterial
fenestrated
lymphatic
venous
venous
lymphatic
fenestrated
arterial
CDH5
PRND GJA4 CXCR4
APLNR PLVAP PLAT
RELN PROX1 CCL21
SPP1 ECM1 OIT3
Rel Expression
1.0
0.5
0.0
−0.5
−1.0
% cells
25
50
75
EPITHELIAL
epithelial
Mesonephric Duct GATA3
Mesonephric Duct
epididymis
male
Mullerian Duct
MullDuct
Epididymis
MesoDuct_CUBN
MesoDuct_GATA3
EPCAM PAX8 EMX2
GATA3 TFAP2A
FXYD2 TFAP2B AMN CUBN SLC3A1
SPINK2 SPAG11B CLDN2
RPS4Y1
WNT7A SCGB2A1 KRT7 KLK11
Rel Expression
2
1
0
−1
% cells
0
25
50
75

Supplementary Fig. 3

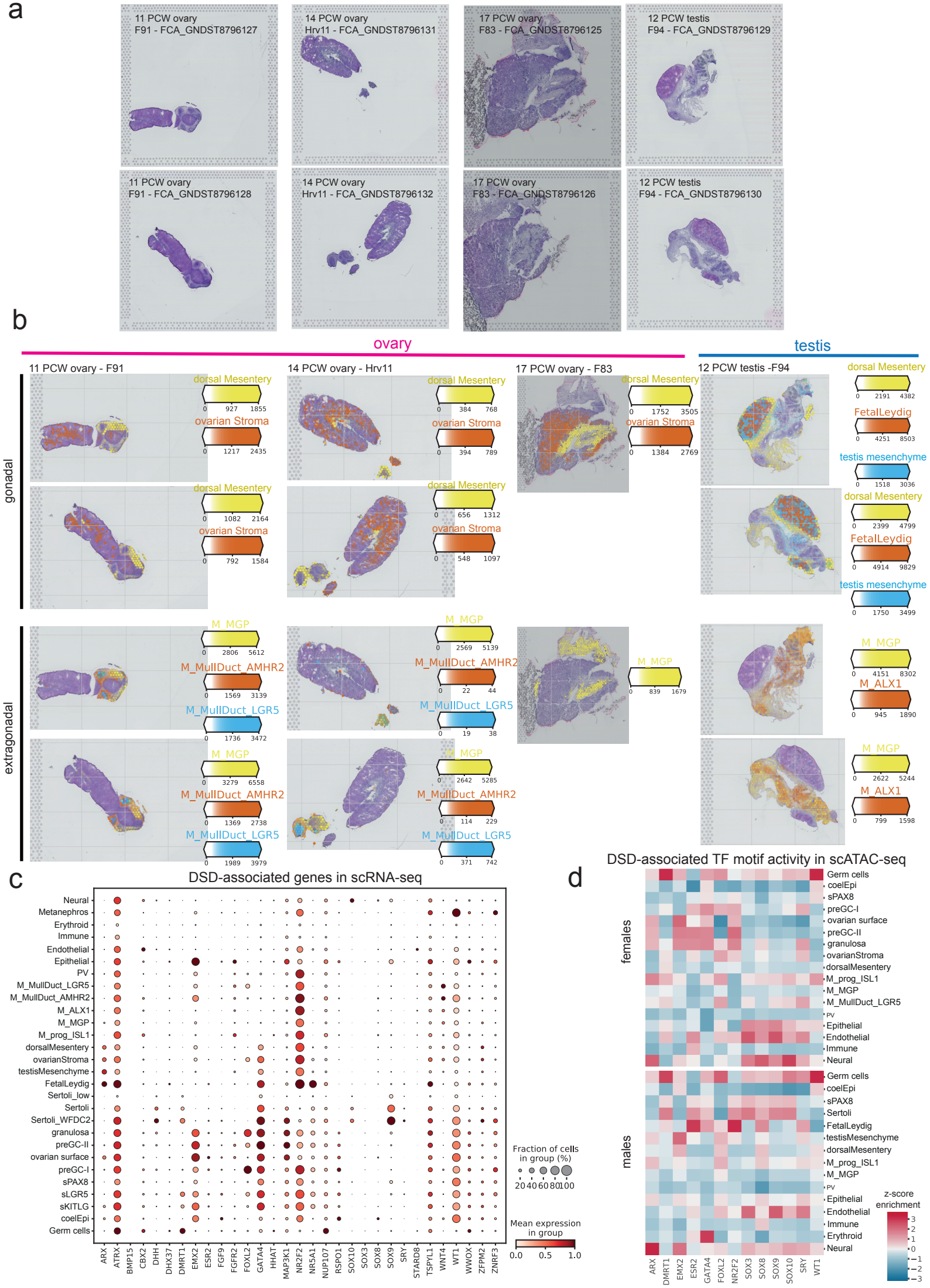

Supplementary Fig. 4

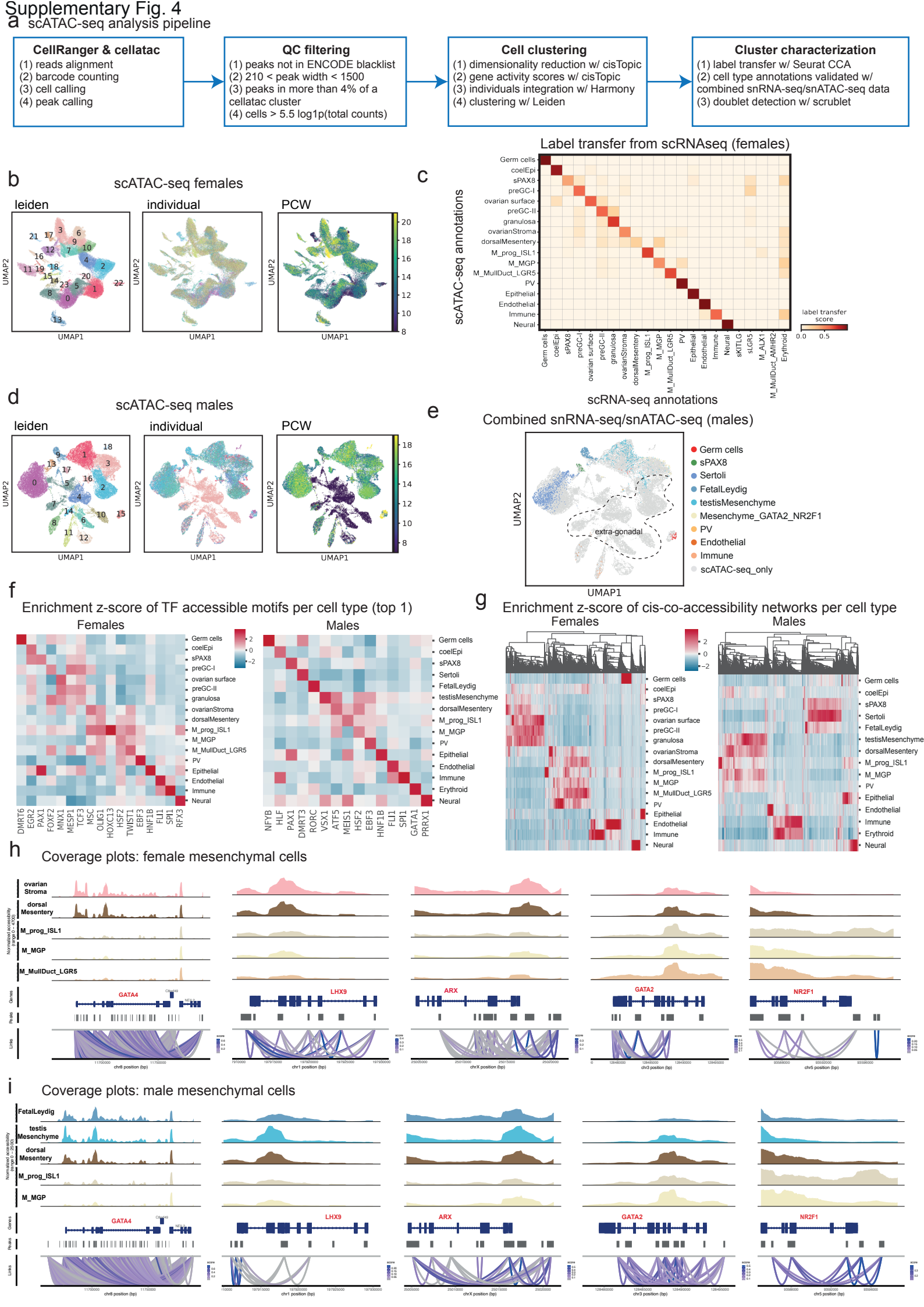

Supplementary Fig. 5

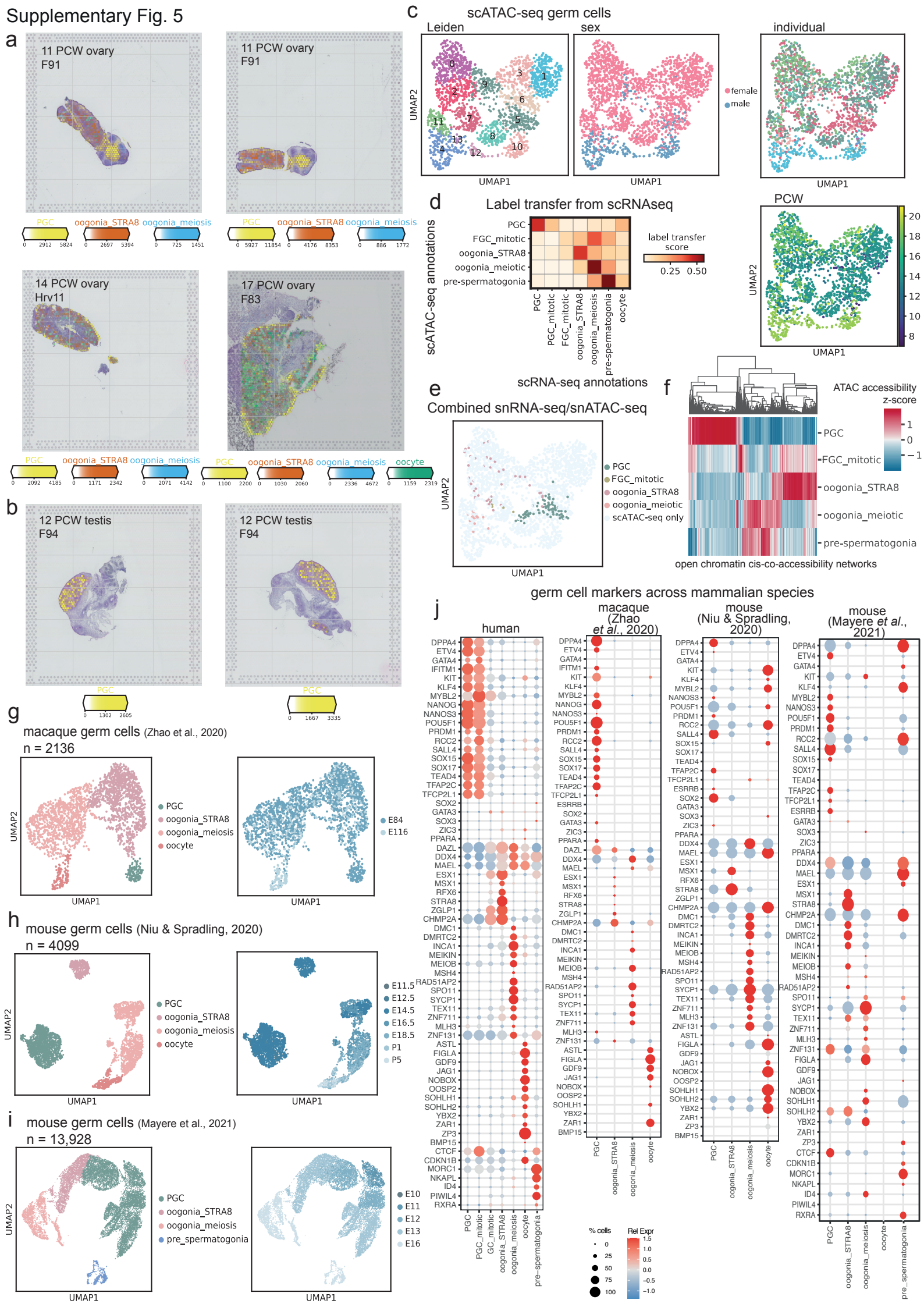

Supplementary Fig. 6

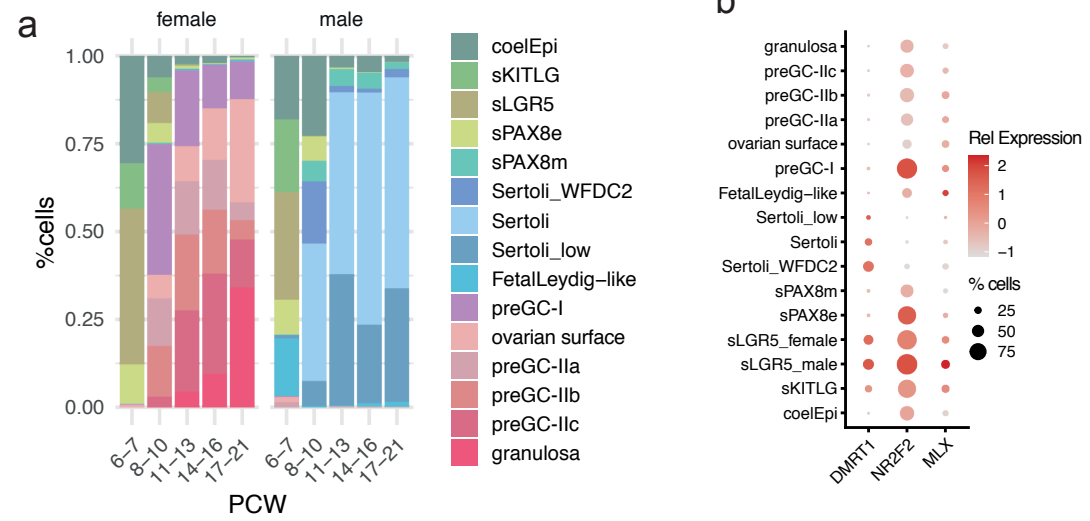

c

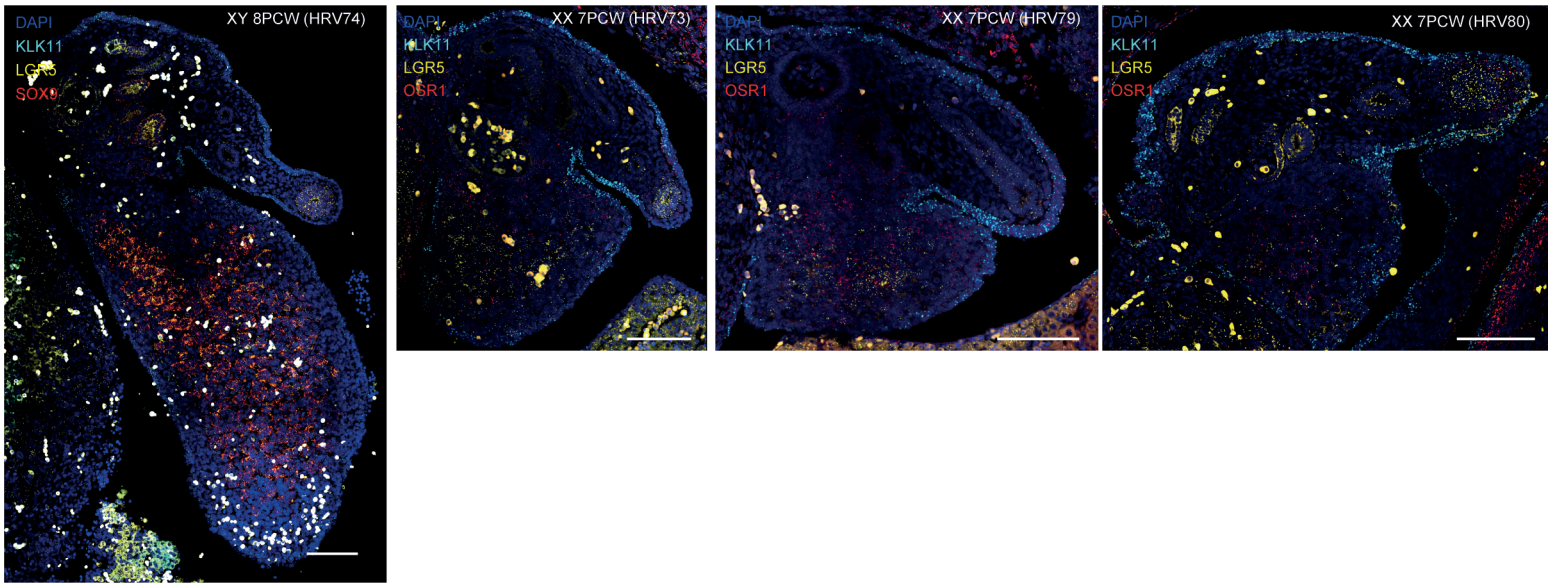

d

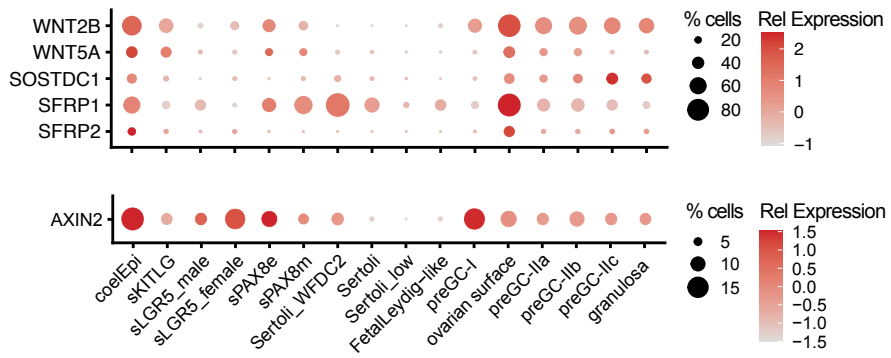

Supplementary Fig. 7

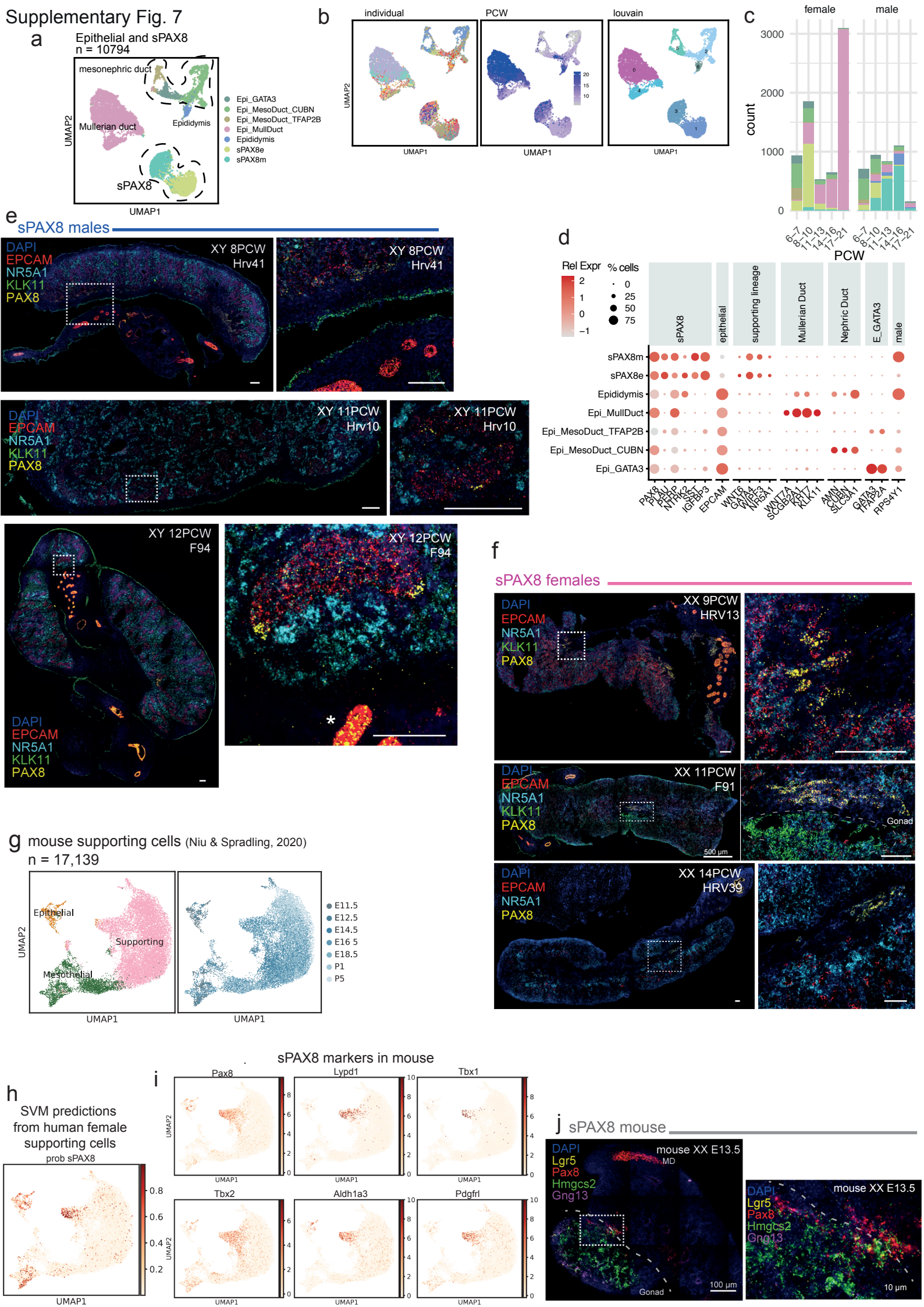

Supplementary Fig. 8

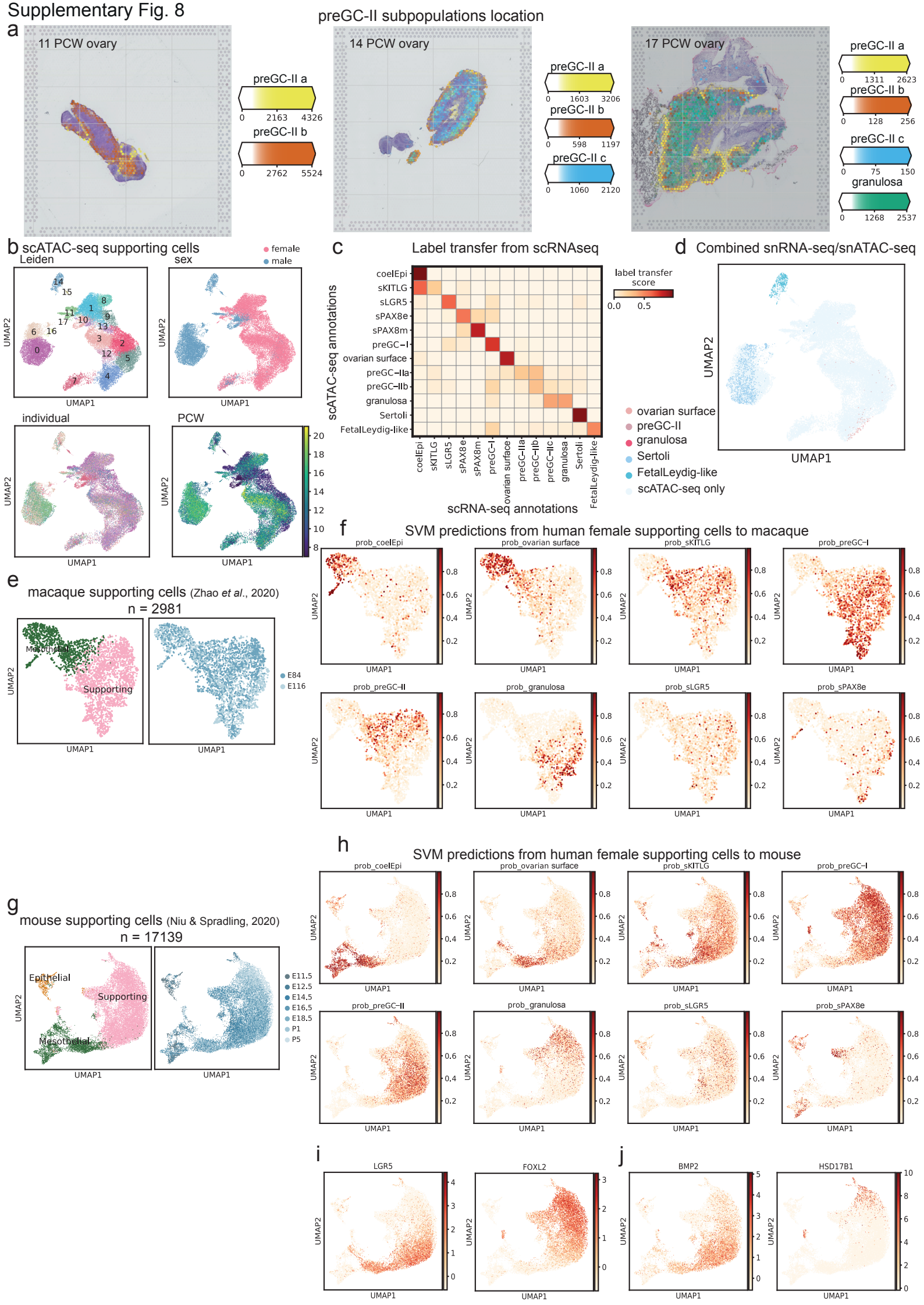

Supplementary Fig. 9

a CD45+ enrichment strategy

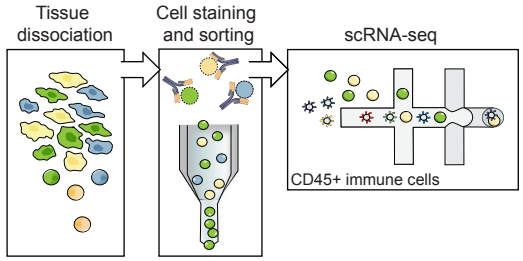

b

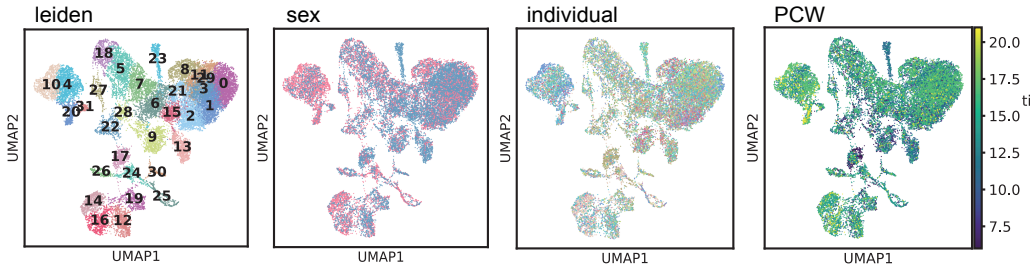

c

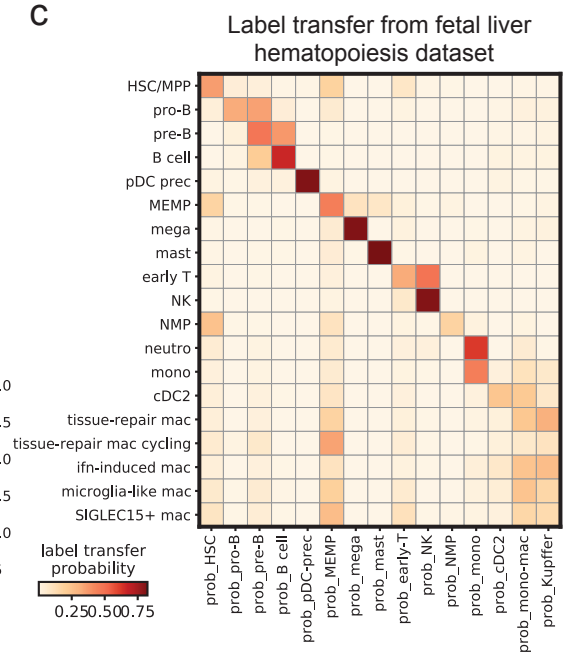

d

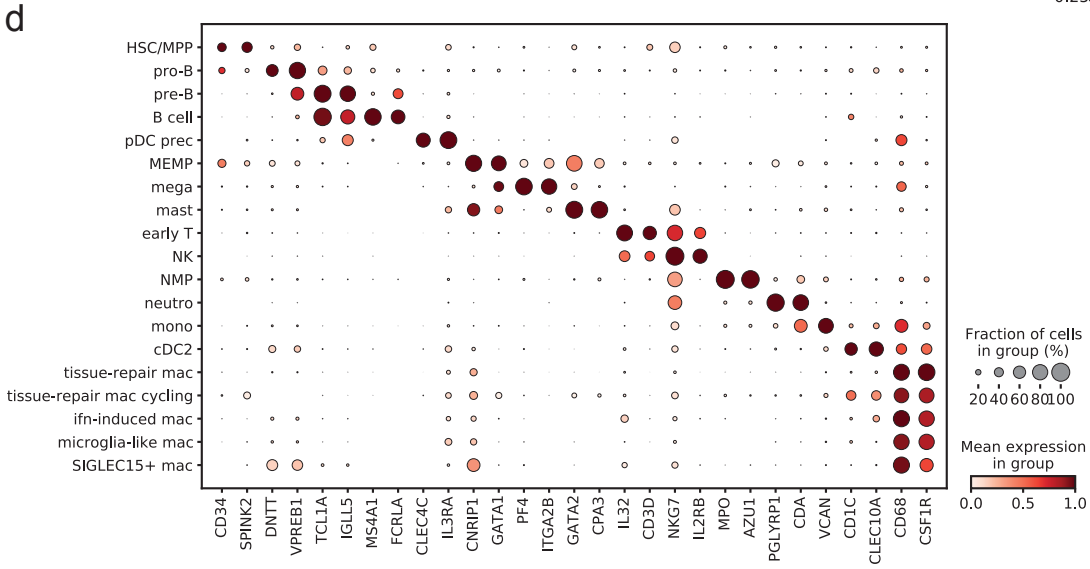

e

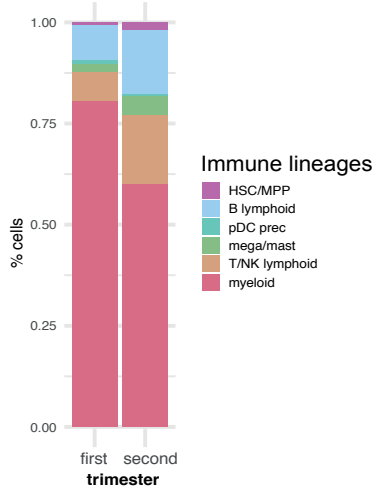

f

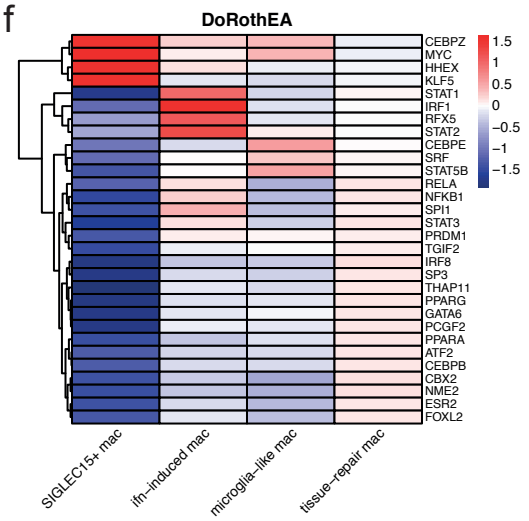

g

Functional enrichment analysis: GO-BP

tissue-repair mac

native	p_value	term_size	intersection_size	recall	name
GO:0050896	0.000000	8621	73	0.008468	response to stimulus
GO:0006954	0.000000	699	16	0.022890	inflammatory response
GO:1901700	0.000054	1669	20	0.011983	response to oxygen-containing compound

ifn-induced mac

native	p_value	term_size	intersection_size	recall	name
GO:0034097	0.000000	1142	35	0.030648	response to cytokine
GO:0034341	0.000000	194	17	0.087629	response to interferon-gamma
GO:0060337	0.000000	82	10	0.121951	type I interferon signaling pathway

microglia-like mac

native	p_value	term_size	intersection_size	recall	name
GO:1904139	0.000134	8	3	0.375000	regulation of microglial cell migration
GO:1903975	0.000850	17	3	0.176471	regulation of glial cell migration
GO:1905523	0.002303	26	3	0.115385	positive regulation of macrophage migration

SIGLEC15+ mac

native	p_value	term_size	intersection_size	recall	name
GO:0030198	0.000157	395	10	0.025316	extracellular matrix organization
GO:0030316	0.001067	95	5	0.052632	osteoclast differentiation
GO:0046849	0.008093	90	4	0.044444	bone remodeling

h

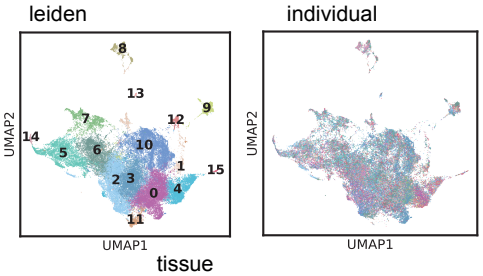

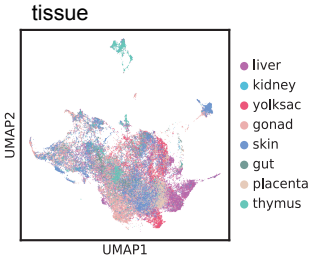

i

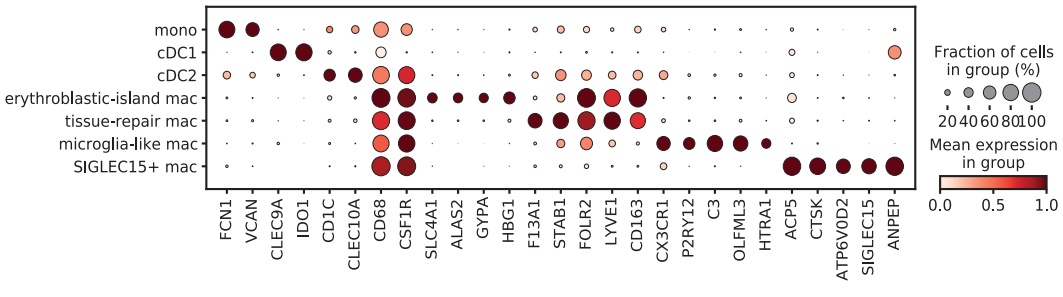

Supplementary Fig. 10

a EPCAM = epithelial (high), Sertoli and germ cells (low), CD68 = macrophage, F13A1 = tissue-repair macrophage

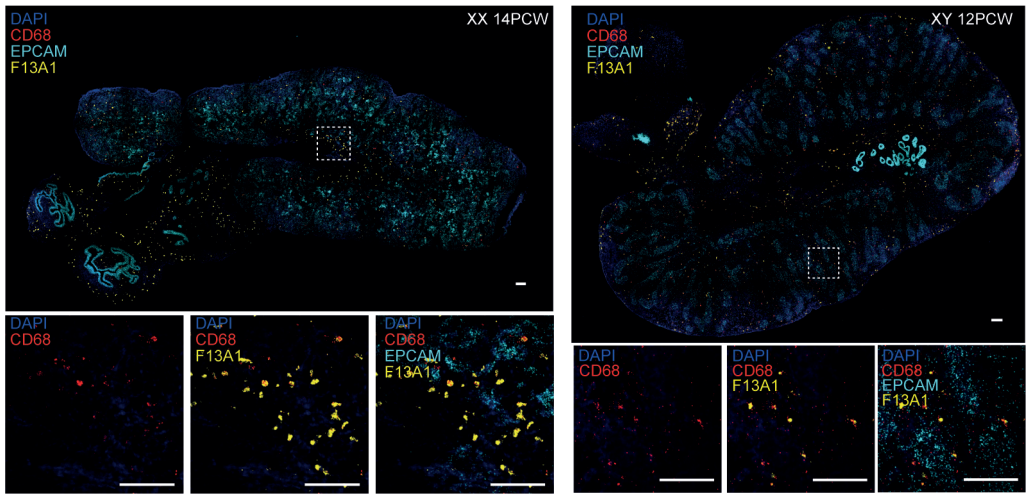

b PDGFRA = mesenchymal, EPCAM = epithelial (high), Sertoli and germ cells (low), CD68 = macrophage, SIGLEC15 = SIGLEC15+ macrophage

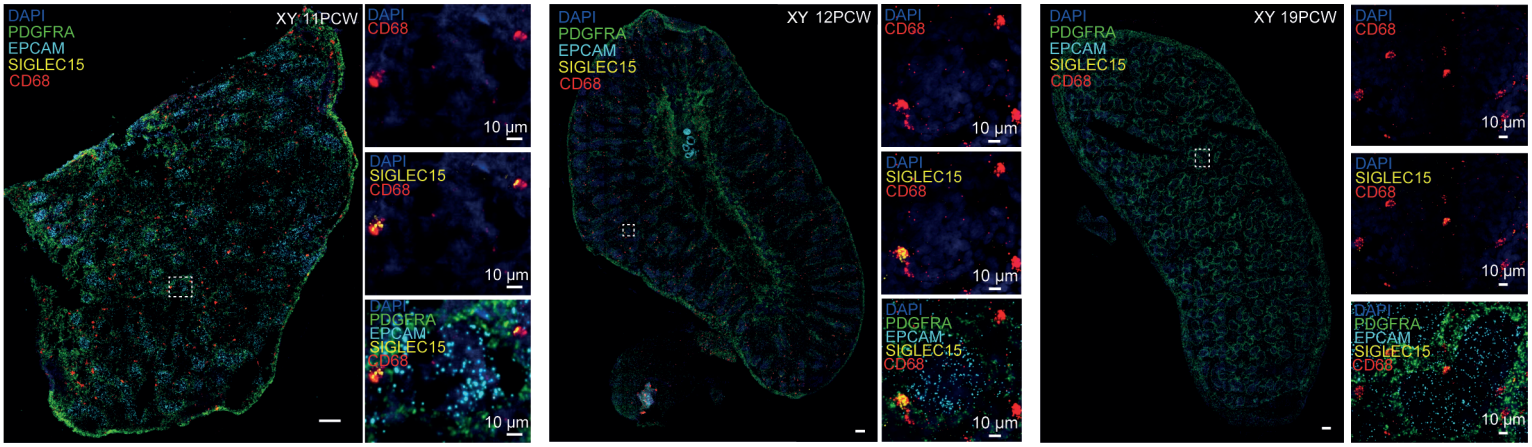

c PDGFRA = mesenchymal, CDH5 = endothelial, CD68 = macrophage, SIGLEC15 = SIGLEC15+ macrophage

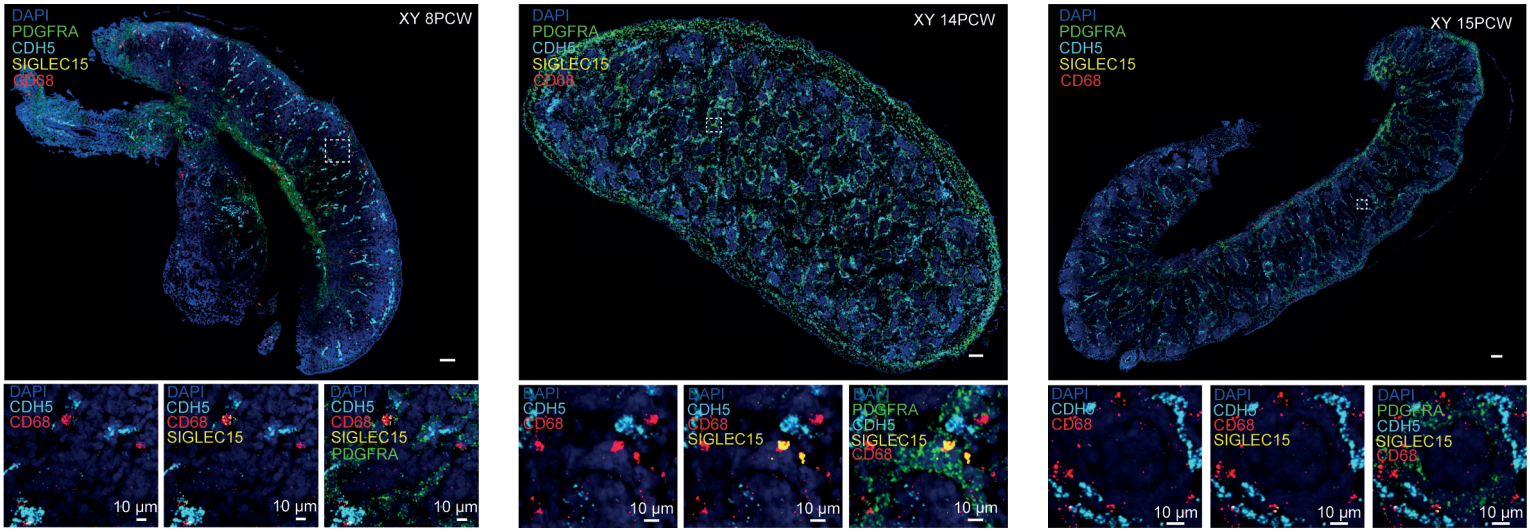

d SOX9 = Sertoli, CD68 = macrophage, P2RY12 = microglia-like macrophage

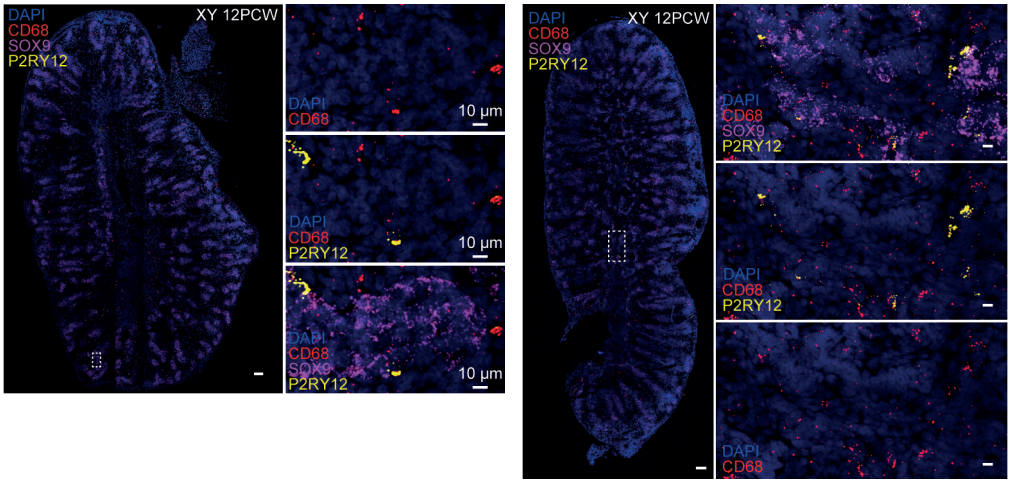

e PDGFRA = mesenchymal, POU5F1 = PGC, CD68 = macrophage, P2RY12 = microglia-like macrophage